iScience

Article

SH2B1 promotes apoptosis in diabetic cataract via p38 MAPK pathway

Graphical abstract

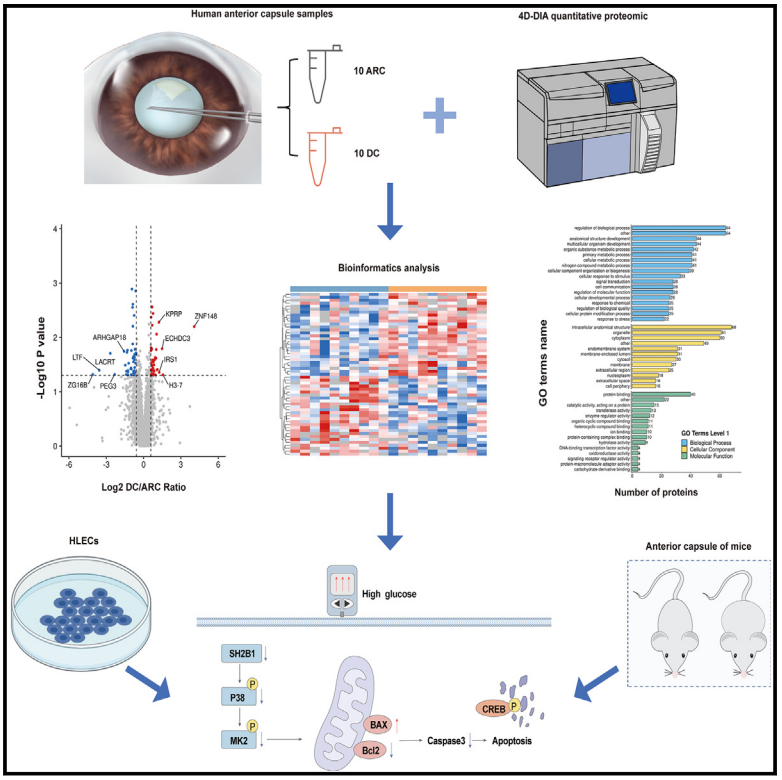

Highlights

- SH2B1 is a key protein in diabetic cataract (DC) progression
- SH2B1 expression is lower in patients with DC and high glucose concentrations
- SH2B1 overexpression lowers apoptosis, promoting cell proliferation and migration
- SH2B1 influences the p38 MAPK pathway, and thereby mitochondrial apoptosis

Authors

Xiaohui Jiang, Liming Xu, Boyue Xu, ..., Yinying Zhao, Nanxin Wu, Yun-e Zhao

Correspondence

zyehzeye@126.com

In brief

Cellular physiology; Molecular biology

Jiang et al., 2025, iScience *28*, 111735
February 21, 2025
https://doi.org/10.1016/j.isci.2024.111735

CellPress

iScience

CellPress
OPEN ACCESS

Article

SH2B1 promotes apoptosis in diabetic cataract via p38 MAPK pathway

Xiaohui Jiang,[1,3] Liming Xu,[1,3] Boyue Xu,[2,3] Haotian Peng,[2] Tonghe Yang,[2] Yinying Zhao,[1] Nanxin Wu,[2] and Yun-e Zhao[1,4,*]

[1]Eye Hospital of Wenzhou Medical University at Hangzhou, 618 East Fengqi Road, Hangzhou 310000, Zhejiang, China
[2]State Key Laboratory of Ophthalmology, Optometry and Vision Science, Eye Hospital, Wenzhou Medical University, Wenzhou 325027, Zhejiang, China
[3]These authors contributed equally
[4]Lead contact
*Correspondence: zyehzeye@126.com
https://doi.org/10.1016/j.isci.2024.111735

SUMMARY

Patients with diabetes face an increased risk of developing cataracts, with unclear mechanisms. Our study illuminates these mechanisms by identifying differentially expressed proteins in the lens anterior capsule of patients with diabetic cataract (DC) and age-related cataract using quantitative proteomics. We found SH2 domain-containing adapter protein B1 (SH2B1) to be crucial in DC progression. Reduced SH2B1 expression was confirmed through PCR and western blotting in patient samples, diet-induced obese mice, and high-glucose (HG)-cultured human lens epithelial cells. Under HG conditions, cell proliferation decreased, while migration and apoptosis, alongside changes in Bcl2 and caspase-3 expression, increased. Overexpressing SH2B1 alleviated these changes and influenced the p38 mitogen-activated protein kinase (MAPK) signaling pathway. This suggests SH2B1 and the p38 MAPK pathway as significant in DC pathogenesis and potential therapeutic targets. Clinically, this could lead to therapies aimed at halting or slowing DC progression.

INTRODUCTION

The global prevalence of diabetes is rising. According to the International Diabetes Federation's 2021 report, there are over 530 million individuals aged 20–79 with type 2 diabetes (T2D) worldwide. This includes a growing number of younger individuals.[1] Diabetic cataract (DC) is one of the most common ocular complications of diabetes, second only to diabetic retinopathy. It occurs approximately five times more frequently in patients with diabetes than in those without and often presents at an earlier age.[2] The current treatment options for cataracts primarily involve surgical removal and intraocular lens implantation. However, surgery of DC is associated with a high risk of complications, such as macular edema, the progression of retinopathy, and iris neovascularization.[3] Biochemical defects in the eyes of patients with diabetes affect the metabolism of lens epithelial cells and increase the risk of DC. Numerous studies have shown that there are high concentrations of inflammatory substances in aqueous humor (AH), defects in antioxidant defense mechanisms, and high concentrations of advanced glycation end products in patients with diabetes.[4–7] *In vitro* experiments using human lens epithelial cells (HLECs) cultured under high-glucose (HG) conditions have demonstrated greater apoptosis,[8] inhibition of autophagy,[9] and epithelial-mesenchymal transition).[10,11] However, there have been few studies of the long-term changes in lens epithelial cells in the AH.

Proteomic sequencing has been used in a variety of ophthalmic studies to reveal differences in the expression patterns of proteins within cells.[12] Titz et al. used proteomics to compare the differences in the expression of AH proteins in the presence of ocular confounders and evaluated their effects on the characteristics of retinal diseases.[13] In addition, Gong et al. revealed the critical role of macrophages in primary acute angle-closure glaucoma induced by severe acute respiratory syndrome coronavirus 2 through the proteomic analysis of AH.[14] They obtained the anterior capsule (AC) membranes of the lenses of patients with cataracts, which are composed of the epithelial cells and their secreted proteins. A series of abnormally expressed proteins were identified by high-throughput proteomic analysis in patients with DC. However, a study of the functional implications of differential protein enrichment between patients with DC and those with age-related cataract (ARC) would help identify the complex signal transduction networks that underpin these pathologies in cells.

In the present study, we used proteomic analysis to identify 85 differentially expressed proteins (DEPs) in the AC of lenses from patients with DC and ARC. We identified dysregulation of the key protein SH2 domain-containing adapter protein B1 (SH2B1) and the downstream p38 mitogen-activated protein kinase (MAPK) signaling pathway in both HG and normal environments using HLECs, diet-induced obesity (DIO) mice, and human-derived AC samples. Furthermore, SH2B1 knockdown increased the sensitivity of HLECs to apoptotic stimuli, whereas overexpression enhanced the ability of HLECs to resist apoptosis. This suggests

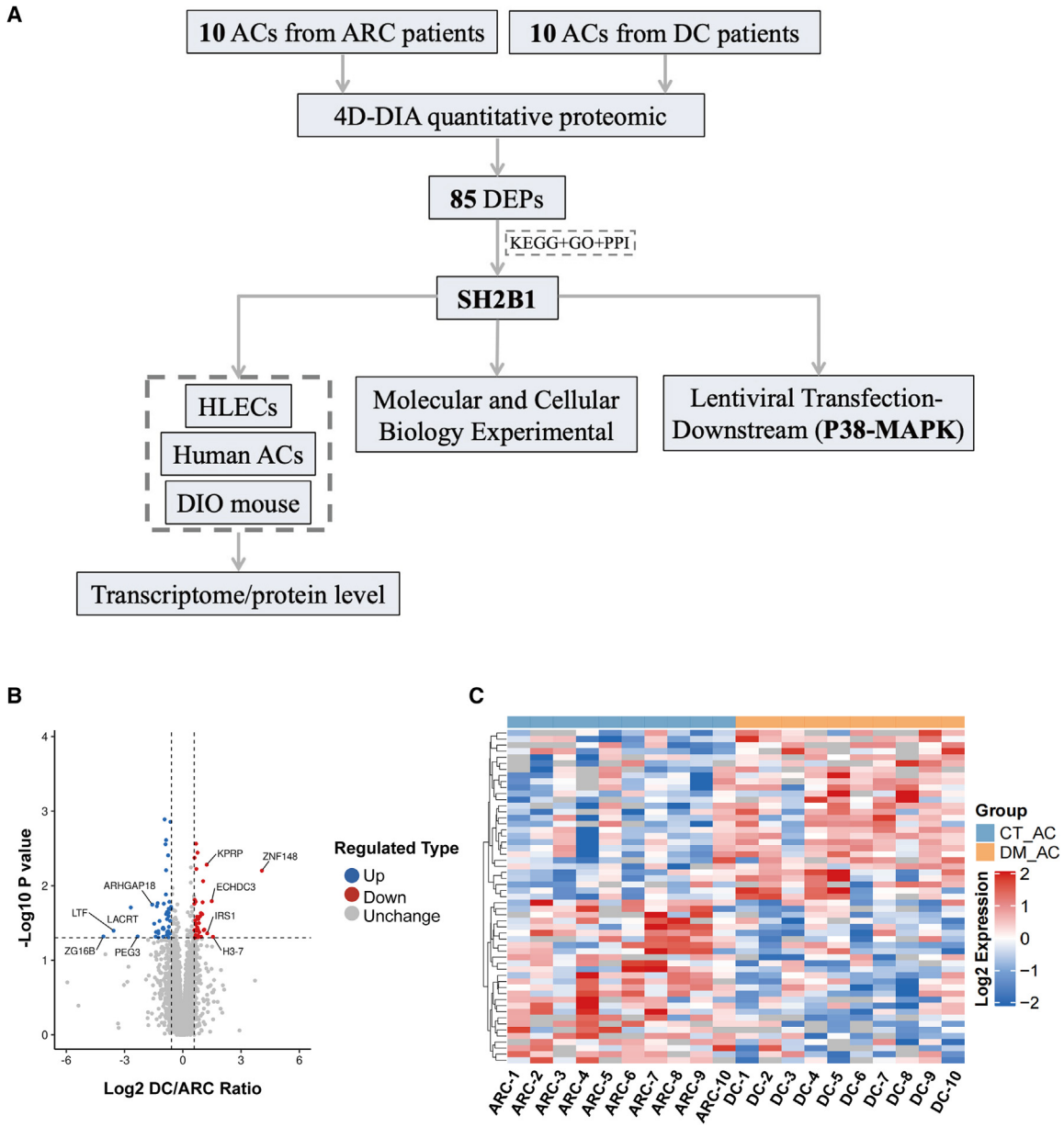

Figure 1. Proteomic analysis of AC in patients with ARC and DC

(A) Schematic diagram of the quantitative proteomic analysis workflow.

(B) Volcano plot of the DEPs for ARC vs. DC in the AC, with thresholds of an FC $\geq$ 1.50 or $\leq$2/3, with $p < 0.05$.

(C) Heatmap showing the DEPs for ARC vs. DC. AC, anterior capsule; ARC, age-related cataract; DC, diabetic cataract; DEPs, differentially expressed proteins; FC, fold change.

that SH2B1 may represent a novel target for the prevention and treatment of DC.

RESULTS

Proteomic characteristics of the ACs from patients with DC or ARC

A flowchart for the present study is shown in Figure 1A. Detailed clinical information regarding the participants, including their age and sex, is presented in Table 1. The mean ages of the 10 patients with ARC and the 10 with DC were 71.30 ± 11.38 and 74.90 ± 11.60 years, respectively. The sex distributions of the two groups did not significantly differ. We identified a total of 5,169 proteins (Table S1), of which 85 were statistically significant DEPs (41 upregulated and 44 downregulated). The DEPs are shown in the form of volcano and heatmaps in Table S2 and Figures 1B and 1C, respectively. The results of the parallel response monitoring testing of the DEPs were consistent with the results of

Table 1. Clinical information of all samples used in this study

Patient characteristics	ARC	DC	*p* value
Sex (male/female)	4/6	5/5	0.6733
Age (years)	71.3 ± 11.38	74.9 ± 11.60	0.9331
Age range (years)	62–86	68–88	–

To provide capsule membrane samples before age-related cataract and diabetic cataract patient's age, gender for statistical analysis.
Abbreviations: ARC, age-related cataract; DC, diabetic cataract. Two-tailed Student's t test.

sequencing (Table S3). The volcano plot shows the five proteins that were most significantly upregulated in the DC group: SH2B, THO complex subunit 3, regulator of G-protein signaling 6, keratinocyte proline-rich protein, and U3 small nucleolar RNA-associated protein 15 homolog. The five proteins exhibiting the most significant downregulation were Rho GTPase-activating protein 18 (ARHGAP18), tear-inducing protein (lacritin), lactotransferrin, zymoglobulin 16 homolog B, and glycerol isostearate (PEG3).

Gene Ontology (GO) biologic process and Kyoto Encyclopedia of Genes and Genomes (KEGG) pathway enrichment analysis of all 85 DEPs revealed 12 GO and 6 KEGG pathways that were significantly dysregulated (Tables S4 and S5). The most significantly enriched items in the biological process (BP), molecular function (MF), and cellular component (CC) categories were "negative regulation of endopeptidase activity" (*p* adjusted = 0.0019, seven proteins), "iron chaperone activity" (*p* adjusted = 0.0006, two proteins), and "anaphase-promoting complex" (*p* adjusted = 0.0047, two proteins) (Figure 2A). The "neurotrophin signaling pathway" showed the most significant changes on KEGG analysis, followed by "cell cycle" (*p* adjusted = 0.0143) (Figure 2B). To better understand the relationships between DEPs, we used the STRING database for protein-protein interaction (PPI) analysis. Of the 85 DEPs, 13 were found to interact with other proteins (Figure 2C). In particular, SH2B1 and insulin receptor substrate (IRS1) were found to interact with one another, and therefore these may represent specific biologic markers of or potential targets for the treatment of DC.

SH2B1 downregulation in diabetic cataract: Effects on HLEC proliferation and apoptosis

The analysis of the proteomic results showed that the expression of SH2B1 protein was significantly lower in the ACs of patients with DC. Several important signaling pathways were found to be substantially differently represented on the GO and KEGG analyses, including the MAPK pathway. Furthermore, SH2B1 was found to be centrally located in the PPI network, along with the interacting protein IRS1. On the basis of these findings, we hypothesize that SH2B1 may play a crucial role in the mechanisms of the progression of DC.

The significant 49% reduction in SH2B1 RNA expression in patients with DC compared to patients with ARC ($p < 0.0001$) suggests a potential role of SH2B1 in DC pathogenesis (Figure 3A). In addition, western blot (WB) analysis showed that the expression of SH2B1 protein in the ACs of patients with DC was approximately 25% lower ($p = 0.0301$) (Figures 3B and 3C). We also harvested the ACs from normal and DIO mice and extracted mRNA and protein from these. The expression of SH2B1 mRNA and protein in the ACs of DIO mice was significantly lower than that of the control group, with the SH2B1 protein expression in the ACs of DIO mice being 46% lower ($p = 0.0013$) (Figures 3C and 3D). DIO mice have been widely used in various experiments in diabetes research to mimic the pathophysiological features of human T2D, such as elevated blood glucose and insulin resistance. The decrease in SH2B1 in the AC of DIO mice further demonstrates the effects of ocular hyperglycemic environment on protein levels. We cultured HLECs in media with glucose concentrations of 5.50, 50, 100, and 150 mM, observing significant downregulation of SH2B1 mRNA and protein expression at 100 and 150 mM. Specifically, the protein expression was 26% and 28% lower, respectively ($p < 0.05$), than in cells cultured in low-glucose (5.50 mM) medium. However, there was no significant difference between the 100 and 150 mM groups ($p = 0.9952$) (Figures 3E and 3F). Based on these findings, we designated 100 mM as a HG concentration and 5.50 mM as a normal glucose (NG) concentration for subsequent experiments.

CCK8 analysis revealed declines in cell proliferation on days 1, 2, and 3 of HG culture, with statistically significant differences ($p < 0.0001$) being identified on days 2 and 3 (Figure 4A). The wound healing assay showed a reduction in migration area of at least 50% after 12 h under HG conditions ($p = 0.0025$) (Figures 4B and 4C). Furthermore, we measured the protein expression of caspase-3, a critical protein in apoptosis, and Bcl2, an inhibitor of apoptosis, in HLECs cultured under NG and HG conditions (Figures 4D and 4E) and found that the expression of both under HG conditions was only approximately 20% of that under NG conditions ($p < 0.001$ and $p < 0.0001$, respectively). Other indices of apoptosis were also assessed. The Bcl-2/Bax expression ratio reflects the sensitivity of cells to apoptotic signals, and the P-cAMP response element-binding protein (CREB)/CREB ratio reflects the response of cells to survival and death signals. Both ratios were lower under HG conditions (Figures 4F–4J). These data are consistent with previously reported findings that a HG concentration increases apoptosis in HLECs.[15,16]

Effects of the overexpression or knockdown of SH2B1 on the proliferation, migration, and apoptosis of HLECs

To investigate the effect of SH2B1 on cell apoptosis, we overexpressed SH2B1 in HLECs using lentiviral vectors (LVs). The efficacy of SH2B1 overexpression (OE-SH2B1) was confirmed by WB analysis (Figures 5A and 5B). The protein expression of SH2B1 was approximately 1.6-fold higher in OE-SH2B1 cells than in control group (negative control [NC]) cells ($p = 0.0013$). CCK8 assays showed that OE-SH2B1 increased HLEC survival under both NG and HG conditions, such that OE-SH2B1 cells showed similar survival under HG conditions as under NG conditions, unlike NC cells. On day 3, the optical densities (ODs) for OE-SH2B1 under HG conditions were 1.4 times higher than those of NC cells ($p < 0.0001$) (Figure 5C). The results of the wound healing experiment showed that the motility of the cells was reduced by culture under HG conditions ($p < 0.001$), whereas the mobility of the OE-SH2B1 cells was only slightly, and not significantly, reduced by HG conditions. In addition, under HG conditions, the motility of both NC and LV-SH2B1 cells was significantly lower ($p = 0.0019$) (Figures 5D and 5E).

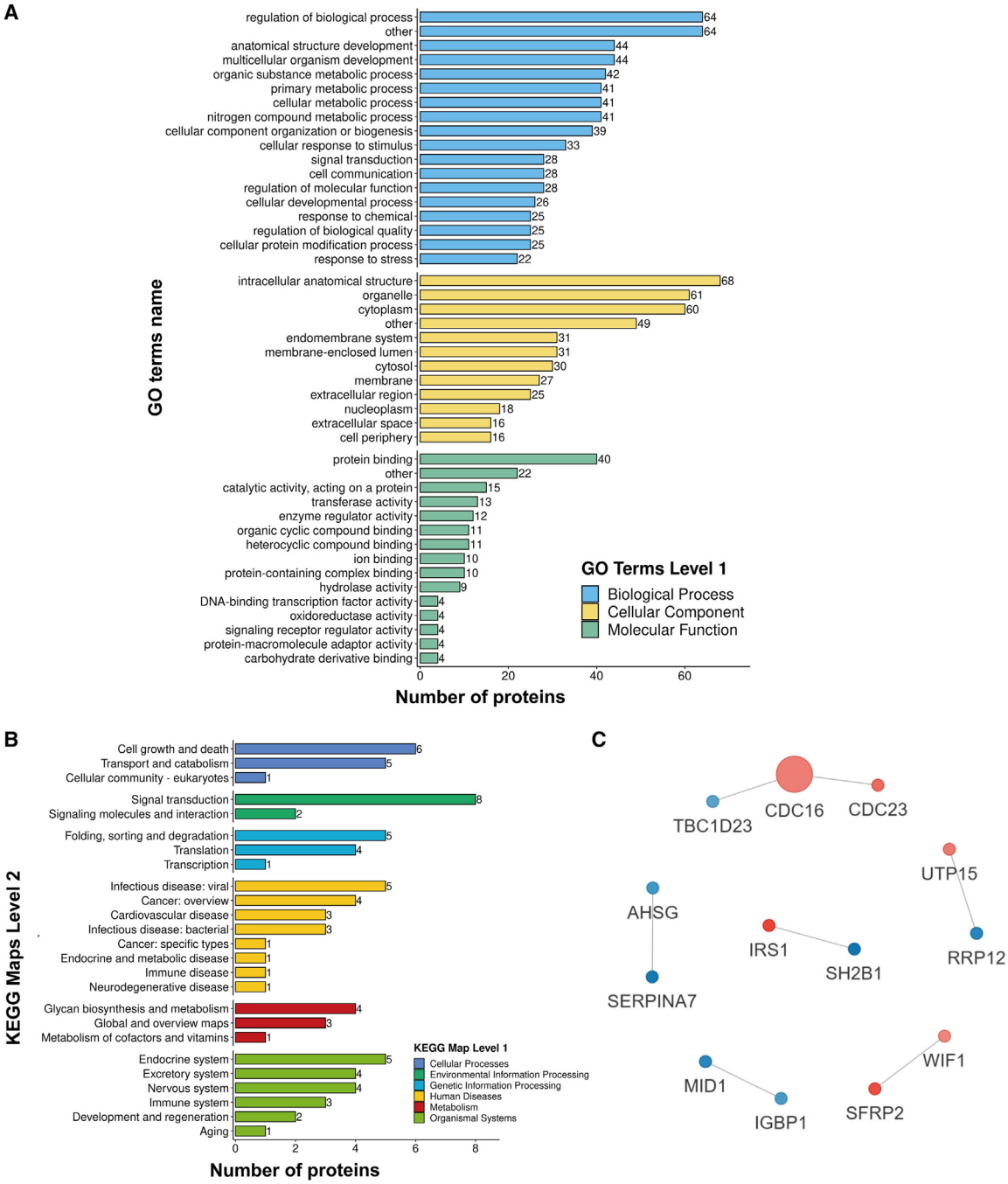

Figure 2. Characterization of the DEPs and PPI in patients with DC

(A) Results of the (A) Gene Ontology (GO) enrichment analysis of DEPs.

(B) Kyoto Encyclopedia of Genes and Genomes (KEGG) pathway analysis of DEPs.

(C) The DEPs were compared with the STRING (v.11.5) protein interaction network database to identify the interactions. Blue: downregulated protein; red: upregulated protein. DC, diabetic cataract; DEPs, differentially expressed proteins.

TUNEL staining, which reveals apoptotic cells, showed that under HG conditions, the proportion of TUNEL-positive cells in OE-SH2B1 cells was significantly lower than that in NC cells (59.0% vs. 13.5%, respectively; $p = 0.0014$) (Figures 6A and 6B). In addition, we measured the expression of apoptosis-related proteins in both groups of cells under NG and HG conditions (Figures 6C and 6D). Notably, the protein expression of Bcl2 and caspase-3 was higher in OE-SH2B1 cells under HG conditions than in NC cells ($p = 0.0065$ and $p < 0.0001$, respectively). In addition, the Bcl2/Bax and p-CREB/CREB ratios in the

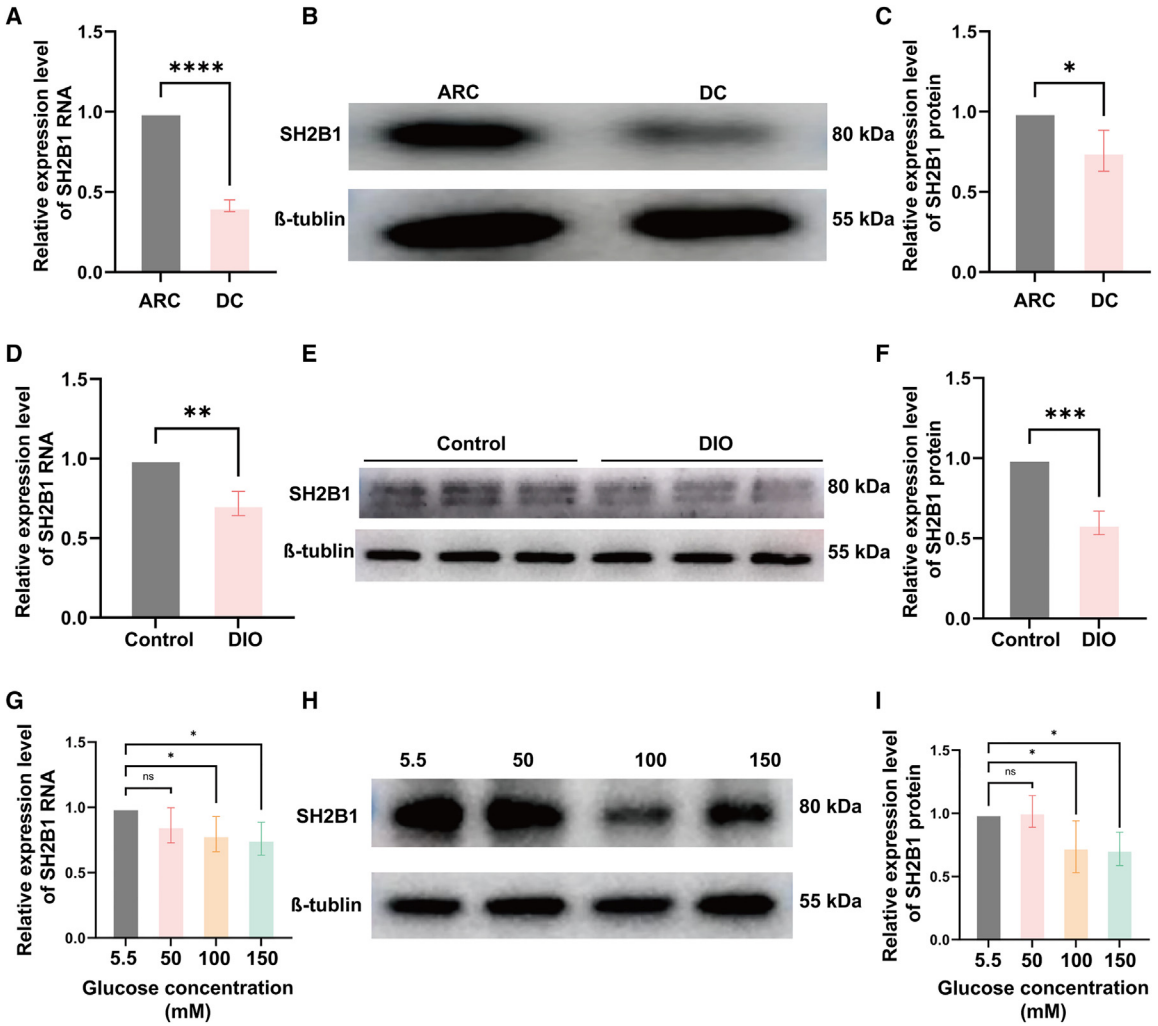

Figure 3. SH2B1 mRNA and protein expression in HLECs cultured in various concentrations of glucose

(A–C) SH2B1 mRNA and protein expression in the anterior capsule of patients with cataract, with or without diabetes.

(D–F) SH2B1 mRNA and protein expression in the lenses of 14-week-old normal and DIO mice.

(G–I) SH2B1 mRNA and protein expression in HLECs cultured in various concentrations of glucose. DC, diabetic cataract; DIO, diet-induced obesity; HLECs, human lens epithelial cells.

Data are represented as mean ± SD ($n = 3$). Data were collected during three independent experiments. $p < 0.05$, $^{**}p < 0.01$, $^{***}p < 0.001$, $^{****}p < 0.0001$. (A, C, D, F) Two-tailed Student's t test; (G, I) two-way ANOVA.

OE-SH2B1 group were 2.2-fold and 1.7-fold higher than those in NC group under HG conditions ($p = 0.0012$ and $p = 0.0002$) (Figures 6E–6H). The total CREB protein expression was also high ($p = 0.0120$) (Figure 6I). Thus, an increase in P-CREB expression following the overexpression of SH2B1 likely increased the expression of anti-apoptotic genes and prolonged cell survival.

We also used small interfering (si) RNA to knock down the SH2B1 gene. si-SH2B1-2 had the best effect, reducing the protein expression of SH2B1 by >80% ($p < 0.001$), and therefore it was used in subsequent experiments (Figures 7A and 7B). CCK8 assays revealed that si-SH2B1-2 cells had poorer cell survival after 2 and 3 days than NC cells (Figure 7C). The wound healing experiment showed that the mobility of si-SH2B1-2 cells was reduced by approximately 30% under HG conditions ($p = 0.0084$) (Figures 7D and 7E). Specifically, the lower SH2B1 expression led to reductions in cell proliferation and migration. Furthermore, the expression of Bcl2 and caspase-3 was lower in si-SH2B1-2 cells, even under NG conditions, than in NC cells (Figures 7F and 7G). The Bcl-2/Bax and P-CREB/CREB ratios were also low, indicating that HLECs show hyperreactivity to death signals and initiate apoptosis when SH2B1 protein expression is low (Figures 7H–7L).

The SH2B1/p38 MAPK/MK2 pathway is involved in the HG-induced apoptosis of HLECs

SH2B1, an integral adapter protein, is pivotal for the phosphorylation and activation of intermediates in a range of receptor-based signaling cascades, and notably those involving Janus

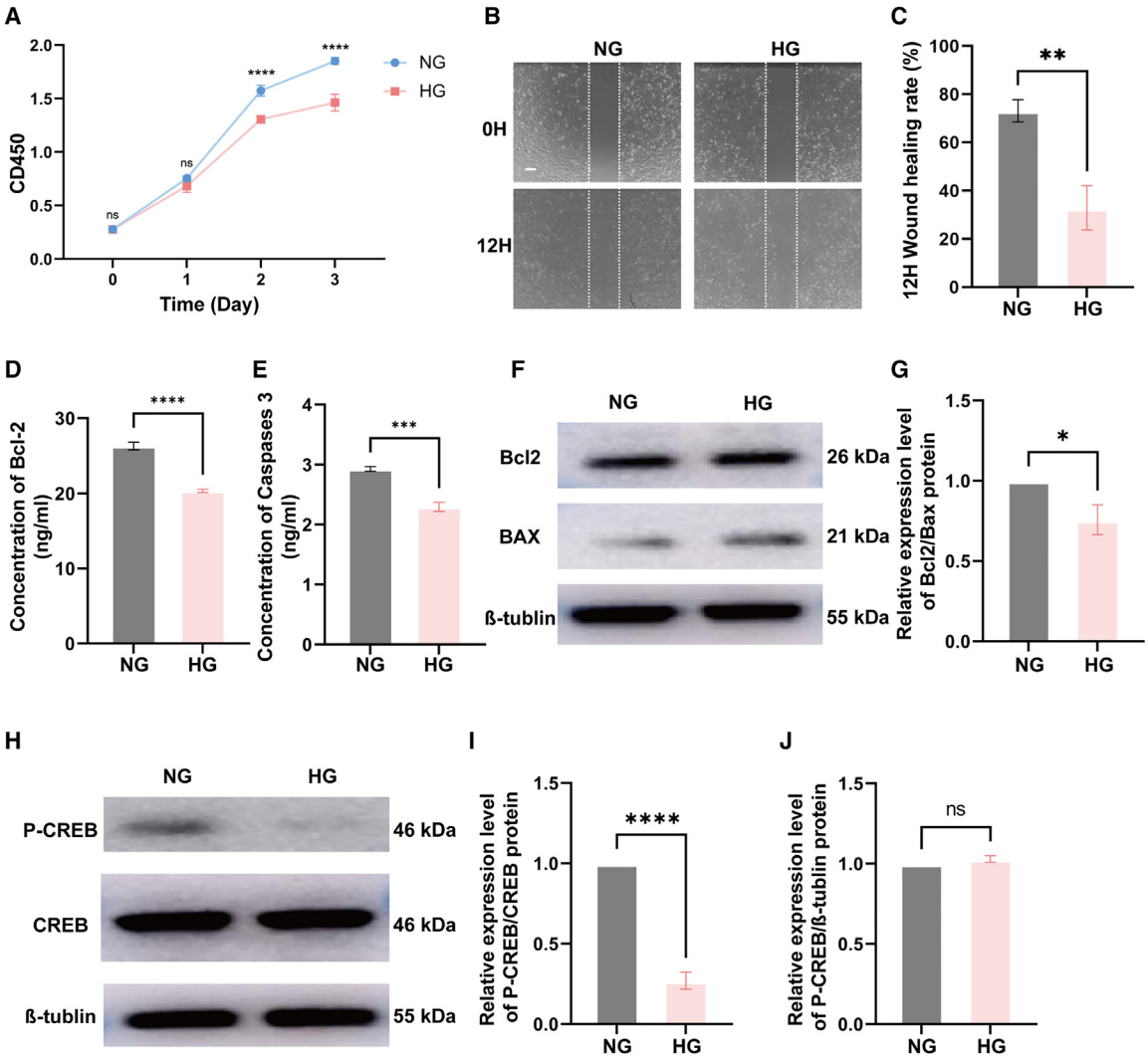

Figure 4. Effects of a high-glucose environment on the proliferation, migration, and apoptosis of HLECs

(A) Proliferation of cells under NG (5.5 mM) (A) and HG (100 mM) conditions after 1, 2, and 3 days.

(B and C) Wound healing rate under NG and HG conditions after 12 h. Scale bar: 200 μm.

(D and E) Expression of Bcl2 and caspase-3 proteins under NG and HG conditions.

(F and G) WB results and analysis of the Bcl2/Bax ratio.

(H–J) WB results and analysis of the P-CREB/CREB and total CREB/β-tubulin ratios. HG, high glucose; NG, normal glucose.

Data are represented as mean ± SD ($n = 3$). Data were collected during three independent experiments. *$p < 0.05$, **$p < 0.01$, ***$p < 0.001$, ****$p < 0.0001$. (A) Two-way ANOVA; (C–E, G, I, J) two-tailed Student's t test.

kinases (JAKs) and the insulin receptor. Using KEGG pathway enrichment analysis, we have demonstrated the position of SH2B1 as a proximal regulator of the MAPK kinase cascade, with implications for the activities of downstream effectors, such as the MAPK-activated protein kinase (MAPKAPK, also termed MK2).[17,18]

Under HG conditions, the phosphorylation of p38 (P-p38) and MK2 (P-MK2) was low in HLECs, whereas the total protein expression was stable. The overexpression of SH2B1 increased P-p38 and P-MK2, whereas SH2B1 knockdown had the opposite effects (Figures 8A–8C). The ratio of P-p38 to p38 (P-p38/p38) was reduced by 32% under HG conditions ($p = 0.0055$). In OE-SH2B1 cells, this ratio was 250% higher ($p = 0.0075$) than that of NC cells, and it was 17% lower ($p = 0.0036$) in si-SH2B1-2 cells. The total p38 protein expression in si-SH2B1-2 cells was 14.30% lower than that in NC cells ($p = 0.0004$) (Figures 8D and 8E). The MK2/MK2 ratio in HG cells was 43.20% lower than that in NG cells ($p = 0.0016$), but was 225.80% higher after SH2B1 overexpression ($p = 0.0484$). Knockdown of SH2B1 reduced MK2 phosphorylation by 17.10% ($p = 0.0386$) (Figures 8F and 8G). To determine whether the inhibition of p38 has effects on SH2B1, we used the p38 inhibitor VX-745. The mRNA expression of SH2B1, p38, MK2, and CREB was measured 24 h after the treatment of NC and OE-SH2B1 cells with VX-745 (0.20 or 1.00 μM, respectively).

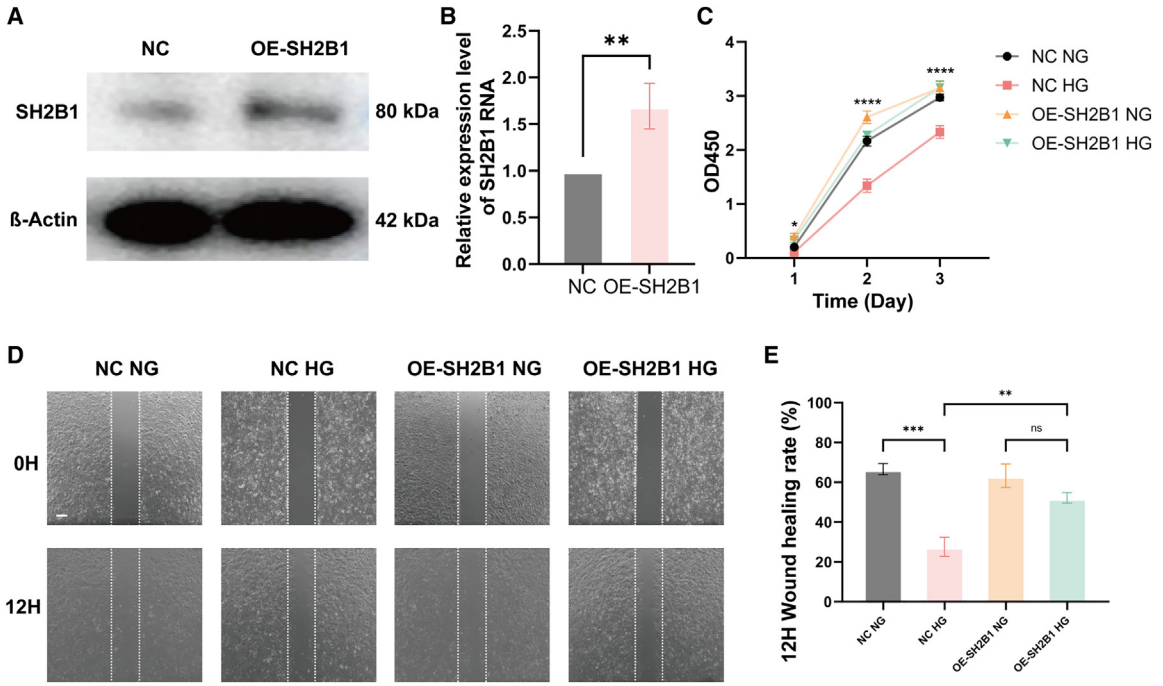

Figure 5. Proliferation and mobility of cells following the overexpression of SH2B1

(A and B) Protein expression following the infection of HLECs with lentivirus expressing SH2B1.

(C) Proliferation rates of SH2B1 overexpressing cells (LV-SH2B1) and control cells (LV-NC) cultured in NG or HG media, assessed after 1, 2, and 3 days, using a CCK8 kit.

(D and E) Wound healing under NG and HG conditions after 12 h for the NC and LV-SH2B1 cells. Scale bar: 200 μm. HG, high glucose; NG, normal glucose. Data are represented as mean ± SD ($n = 3$). Data were collected during three independent experiments. $^{**}p < 0.05$, $^{**}p < 0.01$, $^{***}p < 0.001$, $^{****}p < 0.0001$. (A) Two-tailed Student's t test; (C, E) two-way ANOVA.

The mRNA expression of SH2B1 was not affected in either group of cells, but that of p38, MK2, and CREB were significantly lower (Figure 8H). These findings indicate that SH2B1 regulates the p38 MAPK/MK2 signaling pathway, and thereby affects apoptosis.

DISCUSSION

We have conducted a proteomic analysis of human samples, alongside molecular, cellular, and animal studies. On the basis of the present findings, we have proposed a molecular mechanism for the development of DCs. We have discovered that SH2B1 plays a critical role in the progression of DC via the p38 MAPK signaling pathway. This finding is significant because SH2B1 may represent a molecular target for the prevention of DCs or slowing their progression. To the best of our knowledge, this mechanism has not been previously reported (Figure 9).

Roles of hyperglycemia and SH2B1 in DC pathogenesis

Hyperglycemia has been unequivocally established as a critical risk factor for the premature onset of cataract in patients.[19] However, autophagy,[20,21] fibrosis,[22] apoptosis,[8] and other pathologic processes are also involved in the development of DC. GO analysis of the present proteomic data showed that the proteins of interest are involved in several key biologic processes, including the positive regulation of the MAPK cascade, the regulation of the stress-activated MAPK cascade, and the negative regulation of cell migration. The changes that occur in HLECs during the pathogenesis of DC also involve the enrichment of GO molecular functions such as signaling receptor activity, the regulation of molecular function, and GTPase regulator activity. KEGG analysis showed significant enrichment in signaling pathways, such as cellular aldosterone-regulated sodium reabsorption, O-sugar synthesis, vasopressin-regulated water reabsorption, and neurotrophic factor signaling pathways. In addition, PPI analysis identified 13 protein hub clusters, which included SH2B1, IRS1, CDC23, and secreted frizzled-related protein 2. Of these, SH2B1 and IRS1 appeared to be hub proteins. The low mRNA and protein expression of SH2B1 was identified in DC samples vs. ARC samples. We also identified consistent trends in the expression of SH2B1 in DIO mice and in cells cultured under HG conditions. These findings highlight the pivotal role of hyperglycemia in the pathogenesis of DC and abnormal lens metabolism and show that SH2B1 may play a crucial role in this process.

SH2B1: A conductor of the cellular symphony underpinning metabolism and neurology

SH2B1 is a member of the SH2 family[17] that is principally involved in intracellular signaling, and especially pathways related to insulin signaling. SH2B1 is a key protein in diabetes,[23] insulin resistance,[24,25] and obesity.[26–28] Mice lacking the SH2B1 gene exhibit growth retardation, obesity, and T2D and also have a shorter

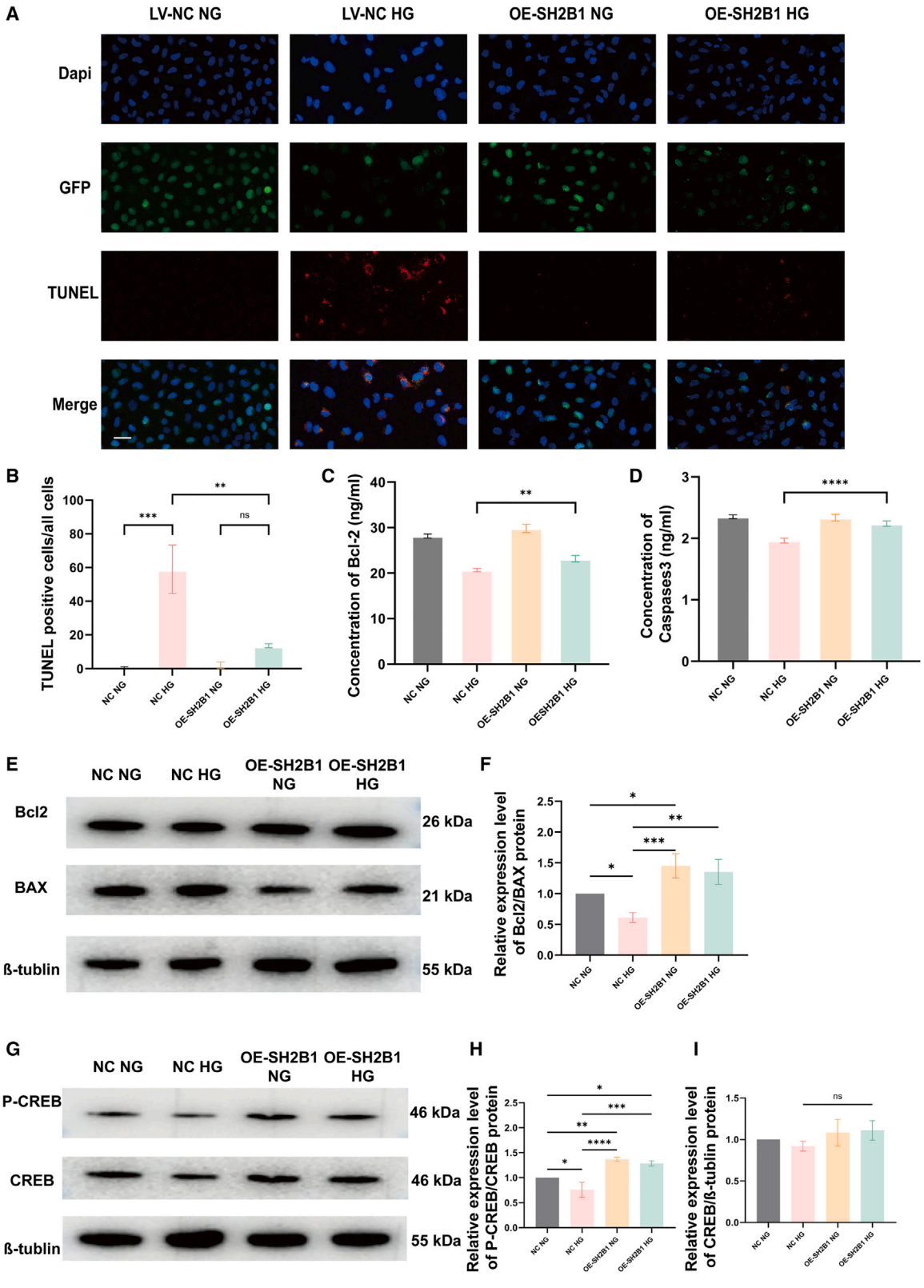

(legend on next page)

lifespan and lower antioxidant capacity. In neuroscience, there has been some progress in the study of SH2B1, which is thought to be involved in neurodegenerative diseases.[27,29] Furthermore, a Mendelian randomization study showed that low SH2B1 expression increased the risk of T2D.[30] Previous studies have shown that SH2B1 is a key component of the sympathetic nervous system/brown adipose tissue/thermogenic axis and is associated with obesity and metabolic disease.[25] It has also been shown to be a positive regulator of the myelination of Schwann cells in peripheral nerves and the maturation of functional neurons derived from induced pluripotent stem cells and induced neurons.[31] Recent studies have shown that the upregulation of SH2B1 also reduces myocardial ischemia/reperfusion-induced inflammation, apoptosis, and increases in reactive oxygen species concentrations.[32] These findings highlight the important role of SH2B1 in both metabolism and neurology. Many previous studies, as well as the present findings, have demonstrated that apoptosis is upregulated in an HG environment, leading to damage to and the death of lens cells,[33] and SH2B1 may affect this process via specific signaling pathways. In the present study, the overexpression of SH2B1 protein increased the anti-apoptotic capacity of HLECs and improved cell survival. Even in an HG environment, TUNEL staining also revealed a decrease in the number of early apoptotic cells. In contrast, the knockdown of SH2B1 protein led to a decrease in the Bcl2/Bax ratio, which reflects greater sensitivity of HLECs to proapoptotic signals and high expression of proapoptotic genes.

Crucial role of SH2B1 in intracellular signaling and the regulation of apoptosis

SH2B1 is important for intracellular signaling. A previous study of non-small cell lung cancer (NSCLC) showed that SH2B1 overexpression causes an increase in the phosphorylation of AKT and mammalian target of rapamycin (mTOR),[34] whereas PTEN knockdown promotes NSCLC cell proliferation.[35] Another study showed that SH2B1 may inhibit apoptosis at least in part through the JAK2/STAT3 pathway.[17,36,37] The results of the present study suggest that the low SH2B1 expression in patients with DC may inhibit the phosphorylation of intermediates in the p38/MK2 signaling pathway through interaction with upstream kinases, such as RAS. As a result, the phosphorylation of transcription factors such as CREB, downstream of the p38/MK2 signaling pathway, is inhibited, thereby increasing the sensitivity of cells to proapoptotic signals. Phosphorylation of CREB is an important way for CREB to regulate transcription. Extracellular signaling pathways modulate the phosphorylation of CREB to activate the transcription of various target genes. Importantly, the phosphorylation state of CREB is deeply connected to apoptosis. By activating anti-apoptotic genes such as Bcl-2 and Bcl-xL, phosphorylated CREB promotes cell survival and provides protection against cellular stress and damage.[38] Despite the known roles of CREB in apoptosis, specific mechanisms by which this occurs in DC remain unreported. A deeper understanding of the mechanism by which SH2B1 regulates the p38/MK2 signaling pathway and the role of CREB in HLECs will not only help with the characterization of the complex regulation of apoptosis but may also provide targets for the development of therapies.

In conclusion, the SH2B1/p38 MAPK signaling pathway plays an important role in the apoptosis of HLECs induced by HG. A deeper understanding of its regulatory role should aid the identification of inhibitors of HLEC apoptosis. This may provide potential novel therapeutic approaches to DC therapy, and this pathway may also become one of the key targets for cataract prevention in patients with obesity or metabolic disease.

Limitations of the study

The present study had some limitations. First, the human AC samples were too small to obtain enough primary cells for experiments. Second, there is a lack of methods to investigate the regulation of gene expression *in vivo* in lens cells, preventing further investigations into the effects of the level of SH2B1 expression on DC.

RESOURCE AVAILABILITY

Lead contact

Further information and requests for resources and reagents should be directed to and will be fulfilled by the lead contact, Yun-e Zhao (zyehzeye@163.com).

Materials availability

This study did not generate new unique reagents and all materials in this study are commercially available.

Data and code availability

- Proteomics data have been deposited at PRIDE and are publicly available as of the date of publication. Accession numbers are listed in the key resources table.
- This paper does not include original code.
- Any additional information required to reanalyze the data reported in this paper is available from the lead contact upon reasonable request.

ACKNOWLEDGMENTS

We thank Mark Cleasby, PhD, from Liwen Bianji (Edanz) (www.liwenbianji.cn) for editing the language of a draft of this manuscript. The study was funded by the National Natural Science Foundation of China (grant no. 82371042). The funder had no role in the design or conduct of the study; the collection, management, analysis, or interpretation of the data; the preparation, review, or approval of the manuscript; or the decision to submit the manuscript for publication.

Figure 6. The overexpression of SH2B1 prevents the apoptosis induced by HG conditions

(A and B) TUNEL staining (red) was used to identify apoptosis in NC and OE-SH2B1 cells under NG and HG conditions.

(C and D) Expression of Bcl2 and caspase-3 proteins in NC and OE-SH2B1 cells under NG and HG conditions.

(E and F) Bcl2/BAX protein expression ratio in NC and OE-SH2B1 cells under NG and HG conditions.

(G–I) P-CREB/CREB protein expression ratio and total CREB/β-tubulin expression ratio in NC and OE-SH2B1 cells under NG and HG conditions. HG, high glucose; NG, normal glucose.

Data are represented as mean ± SD ($n = 3$). Data were collected during three independent experiments. *$p < 0.05$, **$p < 0.01$, ***$p < 0.001$, ****$p < 0.0001$. (B–D) Two-way ANOVA; (F, H, I) two-tailed Student's t test.

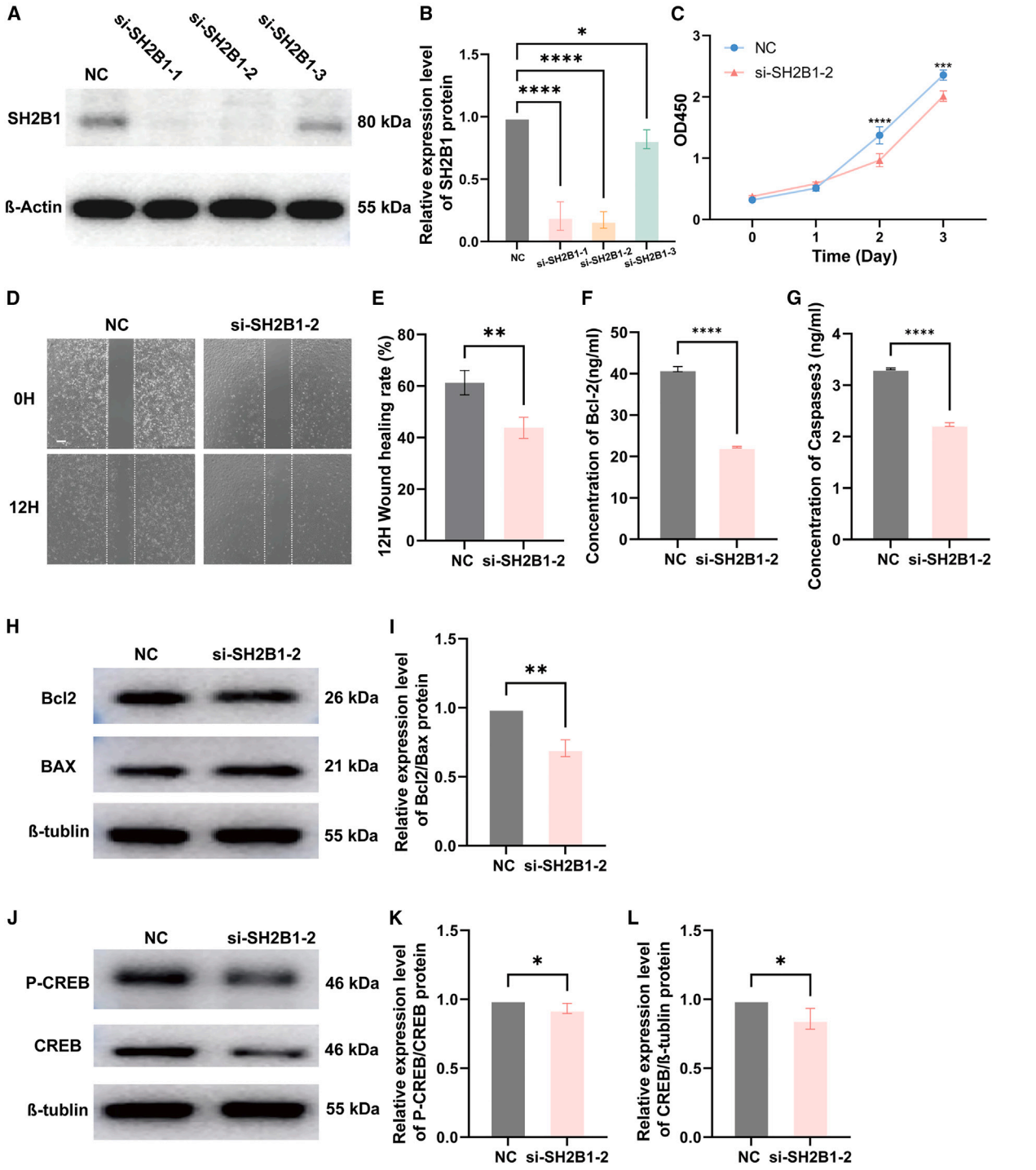

Figure 7. Effects of knocking down SH2B1 on the proliferation, migration, and apoptosis of HLECs

(A and B) Expression of SH2B1 protein after the lentivirus infection of HLECs.

(C) Proliferation rate of each group of cells assessed using a CCK8 kit.

(D and E) Motility of HLECs after knocking down SH2B1 protein. Scale bar: 200 μm.

(F and G) Expression of Bcl2 and caspase-3 proteins in NC and si-SH2B1-2 cells under NG conditions.

(H and I) Bcl2/BAX protein expression ratio in NC and si-SH2B1-2 cells under NG conditions.

(J–L) P-CREB/CREB and total CREB/β-tubulin protein expression ratios for NC and si-SH2B1-2 cells under NG conditions. NG, normal glucose.

Data are represented as mean ± SD ($n = 3$). Data were collected during three separate experiments. *$p < 0.05$, **$p < 0.01$, ****$p < 0.0001$. (B, C) Two-way ANOVA; (E–G, I, K, L) two-tailed Student's t test.

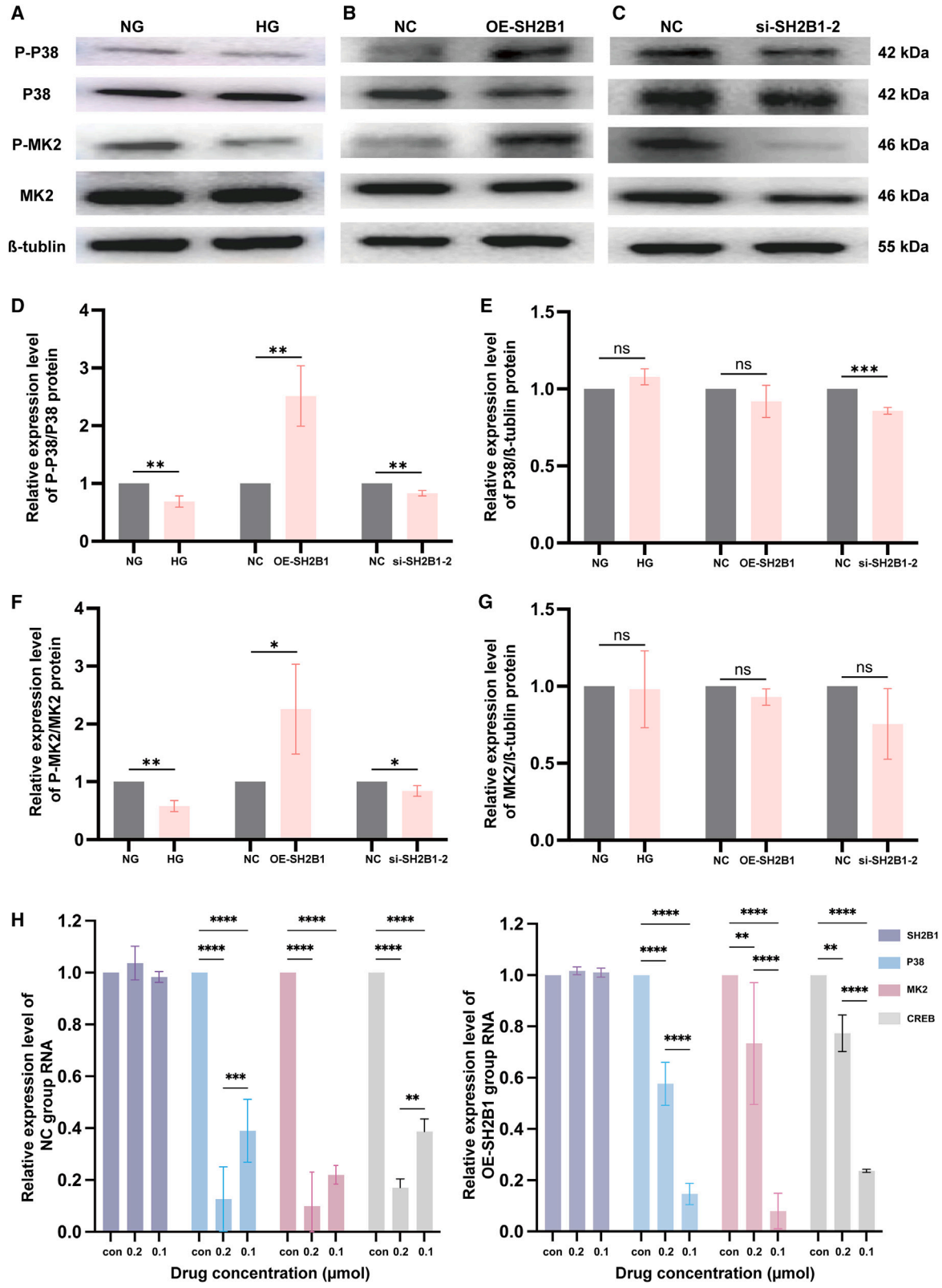

(legend on next page)

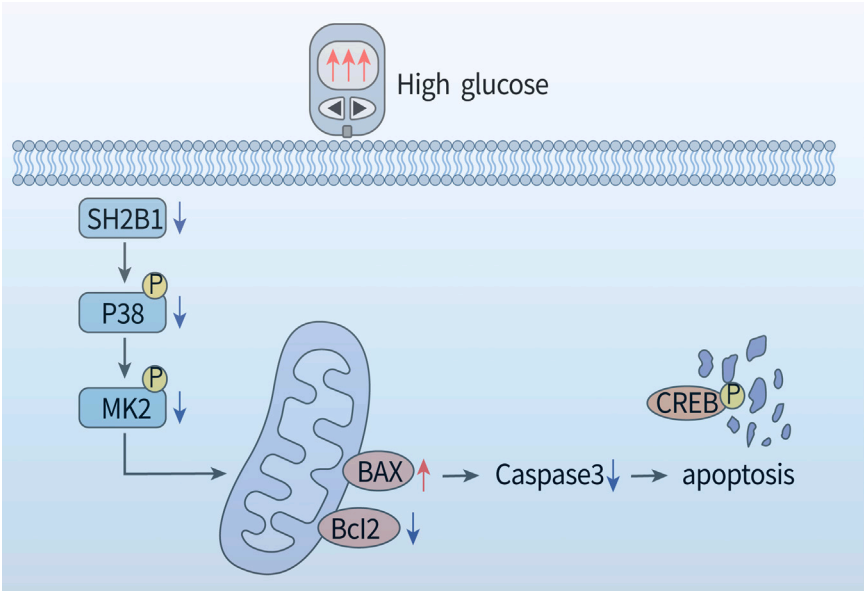

Figure 9. Overview of the p38 MAPK pathway and its relevance

AUTHOR CONTRIBUTIONS

Y.-e.Z. had full access to all of the data in the study and takes responsibility for the integrity of the data and the accuracy of the data analysis. X.J., L.X., and B.X. contributed equally to the work and should be regarded as co-first authors.

Concept and design, Y.-e.Z.; acquisition, analysis, or interpretation of data, X.J., L.X., B.X., T.Y., H.P., N.W., Y.Z., and Y.-e.Z.; drafting of the manuscript, X.J., L.X., and B.X.; critical revision of the manuscript for important intellectual content, Y.-e.Z., X.J., L.X., and B.X.; statistical analysis, X.J., L.X., and B.X.; funding acquisition, Y.-e.Z.; supervision, Y.-e.Z.

DECLARATION OF INTERESTS

The authors declare no competing interests.

STAR★METHODS

Detailed methods are provided in the online version of this paper and include the following:

- KEY RESOURCES TABLE
- EXPERIMENTAL MODEL AND SUBJECT DETAILS
  - Study participants and samples
  - Cell lines
  - Animals
- METHOD DETAILS
  - Sequencing and analysis
  - Parallel response monitoring (PRM) analysis
  - Functional analysis
  - Cell culture and transfection
  - Quantitative polymerase chain reaction (q-PCR)
  - Western blotting (WB)
  - Analysis of cell viability using a cell counting Kit-8 (CCK-8)
  - Wound healing assay
  - Elisa
  - TUNEL fluorescence staining
- QUANTIFICATION AND STATISTICAL ANALYSIS

SUPPLEMENTAL INFORMATION

Supplemental information can be found online at https://doi.org/10.1016/j.isci.2024.111735.

Received: August 7, 2024
Revised: October 14, 2024
Accepted: December 30, 2024
Published: January 2, 2025

REFERENCES

1. Iacobucci, G. (2023). Challenges in diabetes and obesity: five minutes with... Jonathan Valabhji. Bmj *383*, 2831. https://doi.org/10.1136/bmj.p2831.
2. Memon, A.F., Mahar, P.S., Memon, M.S., Mumtaz, S.N., Shaikh, S.A., and Fahim, M.F. (2016). Age-related cataract and its types in patients with and without type 2 diabetes mellitus: A Hospital-based comparative study. J. Pakistan Med. Assoc. *66*, 1272–1276.
3. Patel, J.I., Hykin, P.G., and Cree, I.A. (2006). Diabetic cataract removal: postoperative progression of maculopathy–growth factor and clinical

Figure 8. SH2B1 regulates the p38/MK2 signaling pathway in HLECs

(A–C) Expression and phosphorylation of p38 and MK2 in HG-exposed HLECs in which SH2B1 had been overexpressed or knocked down.
(D and E) Statistical analysis of the P-p38/p38 and total p38/β-tubulin protein expression ratios.
(F and G) Statistical analysis of the P-MK2/MK2 and total MK2/β-tubulin protein expression ratios.
(H) mRNA expression of SH2B1, p38, MK2, and CREB after the treatment of NC and OE-SH2B1 cells with various concentrations of the p38 inhibitor VX-745. Data are represented as mean ± SD ($n = 3$). Data were collected during three independent experiments. $^{*}p < 0.05$, $^{**}p < 0.01$, $^{***}p < 0.001$, $^{****}p < 0.0001$. (D–H) Two-way ANOVA.

analysis. Br. J. Ophthalmol. *90*, 697–701. https://doi.org/10.1136/bjo.2005.087403.

4. Obadă, O., Pantalon, A.D., Rusu-Zota, G., Hăisan, A., Lupuşoru, S.I., Constantinescu, D., and Chiseliţă, D. (2022). Aqueous Humor Cytokines in Non-Proliferative Diabetic Retinopathy. Medicina *58*, 909. https://doi.org/10.3390/medicina58070909.

5. Saucedo, L., Pfister, I.B., Schild, C., Zandi, S., and Garweg, J.G. (2022). Aqueous Humor Apolipoprotein Concentration and Severity of Diabetic Retinopathy in Type 2 Diabetes. Mediat. Inflamm. *2022*, 2406322. https://doi.org/10.1155/2022/2406322.

6. Wang, T., Chen, H., Li, N., Zhang, B., and Min, H. (2024). Aqueous humor proteomics analyzed by bioinformatics and machine learning in PDR cases versus controls. Clin. Proteonomics *21*, 36. https://doi.org/10.1186/s12014-024-09481-w.

7. Xu, W., Liang, Y., Zhu, Y., Sun, T., Yuan, Z., and Han, X. (2023). Proteomic study of aqueous humour in diabetic patients with cataracts by TMT combined with HPLC-MS/MS. BMC Ophthalmol. *23*, 435. https://doi.org/10.1186/s12886-023-03162-2.

8. Wang, Y., Bai, S., Zhang, R., Xia, L., Chen, L., Guo, J., Dai, F., Du, J., and Shen, B. (2021). Orai3 exacerbates apoptosis of lens epithelial cells by disrupting Ca(2+) homeostasis in diabetic cataract. Clin. Transl. Med. *11*, e327. https://doi.org/10.1002/ctm2.327.

9. Li, J., Ye, W., Xu, W., Chang, T., Zhang, L., Ma, J., Pei, R., He, M., and Zhou, J. (2020). Activation of autophagy inhibits epithelial to mesenchymal transition process of human lens epithelial cells induced by high glucose conditions. Cell. Signal. *75*, 109768. https://doi.org/10.1016/j.cellsig.2020.109768.

10. Gao, C., Lin, X., Fan, F., Liu, X., Wan, H., Yuan, T., Zhao, X., and Luo, Y. (2022). Status of higher TGF-β1 and TGF-β2 levels in the aqueous humour of patients with diabetes and cataracts. BMC Ophthalmol. *22*, 156. https://doi.org/10.1186/s12886-022-02317-x.

11. Ma, J., Ye, W., Yang, Y., Wu, T., Wang, Y., Li, J., Pei, R., He, M., Zhang, L., and Zhou, J. (2022). The interaction between autophagy and the epithelial-mesenchymal transition mediated by NICD/ULK1 is involved in the formation of diabetic cataracts. Mol. Med. *28*, 116. https://doi.org/10.1186/s10020-022-00540-2.

12. Lauwen, S., de Jong, E.K., Lefeber, D.J., and den Hollander, A. (2017). Omics Biomarkers in Ophthalmology. Invest. Ophthalmol. Vis. Sci. *58*, Bio88–bio98. https://doi.org/10.1167/iovs.17-21809.

13. Titz, B., Siebourg-Polster, J., Bartolo, F., Lavergne, V., Jiang, Z., Gayan, J., Altay, L., Enders, P., Schmelzeisen, C., Ippisch, Q.T., et al. (2024). Implications of Ocular Confounding Factors for Aqueous Humor Proteomic and Metabolomic Analyses in Retinal Diseases. Transl. Vis. Sci. Technol. *13*, 17. https://doi.org/10.1167/tvst.13.6.17.

14. Gong, Q., Fu, M., Wang, J., Zhao, S., and Wang, H. (2024). Potential Immune-Inflammatory Proteome Biomarkers for Guiding the Treatment of Patients with Primary Acute Angle-Closure Glaucoma Caused by COVID-19. J. Proteome Res. *23*, 2587–2597. https://doi.org/10.1021/acs.jproteome.4c00325.

15. Chen, L., Chen, Y., Ding, W., Zhan, T., Zhu, J., Zhang, L., Wang, H., Shen, B., and Wang, Y. (2022). Oxidative Stress-Induced TRPV2 Expression Increase Is Involved in Diabetic Cataracts and Apoptosis of Lens Epithelial Cells in a High-Glucose Environment. Cells *11*, 1196. https://doi.org/10.3390/cells11071196.

16. Yang, J., Liu, J., Zhao, S., and Tian, F. (2020). Methyladenosine METTL3 Modulates the Proliferation and Apoptosis of Lens Epithelial Cells in Diabetic Cataract. Mol. Ther. Nucleic Acids *20*, 111–116. https://doi.org/10.1016/j.omtn.2020.02.002.

17. Maures, T.J., Kurzer, J.H., and Carter-Su, C. (2007). SH2B1 (SH2-B) and JAK2: a multifunctional adaptor protein and kinase made for each other. Trends Endocrinol. Metabol. *18*, 38–45. https://doi.org/10.1016/j.tem.2006.11.007.

18. Qian, X., Riccio, A., Zhang, Y., and Ginty, D.D. (1998). Identification and characterization of novel substrates of Trk receptors in developing neurons. Neuron *21*, 1017–1029. https://doi.org/10.1016/s0896-6273(00)80620-0.

19. Paisey, R.B., Arredondo, G., Villalobos, A., Lozano, O., Guevara, L., and Kelly, S. (1984). Association of differing dietary, metabolic, and clinical risk factors with microvascular complications of diabetes: a prevalence study of 503 Mexican type II diabetic subjects. II. Diabetes Care *7*, 428–433. https://doi.org/10.2337/diacare.7.5.428.

20. Guo, Z., Ma, X., Zhang, R.X., and Yan, H. (2023). Oxidative stress, epigenetic regulation and pathological processes of lens epithelial cells underlying diabetic cataract. Adv. Ophthalmol. Pract. Res. *3*, 180–186. https://doi.org/10.1016/j.aopr.2023.10.001.

21. Li, J., Sun, Q., Qiu, X., Zhang, J., Zheng, Y., Luo, L., and Tan, X. (2022). Downregulation of AMPK dependent FOXO3 and TFEB involves in the inhibition of autophagy in diabetic cataract. Curr. Eye Res. *47*, 555–564. https://doi.org/10.1080/02713683.2021.2009516.

22. Li, X., Chen, D., Ouyang, B., Wang, S., Li, Y., Li, L., Zhu, S., and Zheng, G. (2023). KLF5/MDM2 Axis Modulates Oxidative Stress and Epithelial-Mesenchymal Transition in Human Lens Epithelial Cells: The Role in Diabetic Cataract. Lab. Invest. *103*, 100226. https://doi.org/10.1016/j.labinv.2023.100226.

23. Al-Eitan, L.N., Aman, H., Alkhatib, R., and Alghamdi, M.A. (2020). Genetic Association of SH2B1 Gene Polymorphisms in Jordanian Arab Patients with Type 2 Diabetes Mellitus. Diabetes Metab. Syndr. Obes. *13*, 1825–1834. https://doi.org/10.2147/dmso.S245843.

24. Song, W., Ren, D., Li, W., Jiang, L., Cho, K.W., Huang, P., Fan, C., Song, Y., Liu, Y., and Rui, L. (2010). SH2B regulation of growth, metabolism, and longevity in both insects and mammals. Cell Metabol. *11*, 427–437. https://doi.org/10.1016/j.cmet.2010.04.002.

25. Jiang, L., Su, H., Wu, X., Shen, H., Kim, M.H., Li, Y., Myers, M.G., Jr., Owyang, C., and Rui, L. (2020). Leptin receptor-expressing neuron Sh2b1 supports sympathetic nervous system and protects against obesity and metabolic disease. Nat. Commun. *11*, 1517. https://doi.org/10.1038/s41467-020-15328-3.

26. Willer, C.J., Speliotes, E.K., Loos, R.J.F., Li, S., Lindgren, C.M., Heid, I.M., Berndt, S.I., Elliott, A.L., Jackson, A.U., Lamina, C., et al. (2009). Six new loci associated with body mass index highlight a neuronal influence on body weight regulation. Nat. Genet. *41*, 25–34. https://doi.org/10.1038/ng.287.

27. Beckers, S., Zegers, D., Van Gaal, L.F., and Van Hul, W. (2011). Replication of the SH2B1 rs7498665 association with obesity in a Belgian study population. Obes. Facts *4*, 473–477. https://doi.org/10.1159/000335305.

28. Shi, J., Long, J., Gao, Y.T., Lu, W., Cai, Q., Wen, W., Zheng, Y., Yu, K., Xiang, Y.B., Hu, F.B., et al. (2010). Evaluation of genetic susceptibility loci for obesity in Chinese women. Am. J. Epidemiol. *172*, 244–254. https://doi.org/10.1093/aje/kwq129.

29. Li, Y., Kim, M.H., Jiang, L., Baron, L., Faulkner, L.D., Olson, D.P., Li, X., Gannot, N., Li, P., and Rui, L. (2024). SH2B1 Defends Against Energy Imbalance, Obesity, and Metabolic Disease via a Paraventricular Hypothalamus→Dorsal Raphe Nucleus Neurocircuit. Adv. Sci. *11*, e2400437. https://doi.org/10.1002/advs.202400437.

30. Hanssen, R., Auwerx, C., Jõeloo, M., Sadler, M.C., Estonian Biobank Research Team, Henning, E., Keogh, J., Bounds, R., Smith, M., Firth, H.V., et al. (2023). Chromosomal deletions on 16p11.2 encompassing SH2B1 are associated with accelerated metabolic disease. Cell Rep. Med. *4*, 101155. https://doi.org/10.1016/j.xcrm.2023.101155.

31. Hsu, Y.C., Chen, S.L., Wang, Y.J., Chen, Y.H., Wang, D.Y., Chen, L., Chen, C.H., Chen, H.H., and Chiu, I.M. (2014). Signaling adaptor protein SH2B1 enhances neurite outgrowth and accelerates the maturation of human induced neurons. Stem Cells Transl. Med. *3*, 713–722. https://doi.org/10.5966/sctm.2013-0111.

32. Wu, G., Liu, Y., Huang, H., Tang, Y., Liu, W., Mei, Y., Wan, N., Liu, X., and Huang, C. (2015). SH2B1 is critical for the regulation of cardiac remodelling in response to pressure overload. Cardiovasc. Res. *107*, 203–215. https://doi.org/10.1093/cvr/cvv170.

33. Lian, L., Le, Z., Wang, Z., Chen, Y.A., Jiao, X., Qi, H., Hejtmancik, J.F., Ma, X., Zheng, Q., and Ren, Y. (2023). SIRT1 Inhibits High Glucose-Induced TXNIP/NLRP3 Inflammasome Activation and Cataract Formation. Invest. Ophthalmol. Vis. Sci. *64*, 16. https://doi.org/10.1167/iovs.64.3.16.

34. Xin, G., Xu-Yong, L., Shan, H., Gang, W., Zhen, C., Ji-Jun, L., Ping, Y., and Man-Hua, C. (2020). SH2B1 protects cardiomyocytes from ischemia/reperfusion injury via the activation of the PI3K/AKT pathway. Int. Immunopharm. *83*, 105910. https://doi.org/10.1016/j.intimp.2019.105910.

35. Wang, S., Zheng, Y., He, Z., Zhou, W., Cheng, Y., and Zhang, C. (2018). SH2B1 promotes NSCLC cell proliferation through PI3K/Akt/mTOR signaling cascade. Cancer Cell Int. *18*, 132. https://doi.org/10.1186/s12935-018-0632-x.

36. Yuan, J., Zeng, L., Sun, Y., Wang, N., Sun, Q., Cheng, Z., and Wang, Y. (2018). SH2B1 protects against OGD/R-induced apoptosis in PC12 cells via activation of the JAK2/STAT3 signaling pathway. Mol. Med. Rep. *18*, 2613–2620. https://doi.org/10.3892/mmr.2018.9265.

37. Doche, M.E., Bochukova, E.G., Su, H.W., Pearce, L.R., Keogh, J.M., Henning, E., Cline, J.M., Saeed, S., Dale, A., Cheetham, T., et al. (2012). Human SH2B1 mutations are associated with maladaptive behaviors and obesity. J. Clin. Invest. *122*, 4732–4736. https://doi.org/10.1172/jci62696.

38. Riccio, A., Ahn, S., Davenport, C.M., Blendy, J.A., and Ginty, D.D. (1999). Mediation by a CREB family transcription factor of NGF-dependent survival of sympathetic neurons. Science *286*, 2358–2361. https://doi.org/10.1126/science.286.5448.2358.

STAR★METHODS

KEY RESOURCES TABLE

REAGENT or RESOURCE	SOURCE	IDENTIFIER
Antibodies		
SH2B1 Polyclonal antibody	Proteintech	Cat# 12226-1-AP; RRID: AB_2877838
Bcl-2 Recombinant Rabbit Monoclonal Antibody	HUABIO	Cat# ET1702-53; RRID: AB_3070315
Bax Recombinant Rabbit Monoclonal Antibody	HUABIO	Cat# ET1603-34; RRID: AB_3069679
CREB Recombinant Rabbit Monoclonal Antibody	HUABIO	Cat# ET1601-15; RRID: AB_3069597
Phospho-Creb (S133) Recombinant Rabbit Monoclonal Antibody	HUABIO	Cat# ET7107-93; RRID: AB_3070798
p38 MAPK Recombinant Rabbit Antibody	HUABIO	Cat# HA722036; RRID: AB_3096629
Phospho-p38 MAPK (Thr180/Tyr182) (D3F9) XP® Rabbit mAb	CST	Cat# 4511; RRID: AB_2139682
MAPKAPK-2 Antibody	CST	Cat# 3042; RRID: AB_10694238
Phospho-MAPKAPK-2 (Thr334) (27B7) Rabbit mAb	CST	Cat# 3007; RRID: AB_490936
Beta Tubulin Mouse mAb	Nature Bioscience	Cat# MA0002; RRID: AB_2924356
beta Actin Mouse Monoclonal Antibody	HUABIO	Cat# EM21002; RRID: AB_2819164
goat anti-mouse IgG (H + L), HRP conjugate	Proteintech	Cat# SA00001-1
goat anti-Rabbit IgG (H + L), HRP conjugate	Proteintech	Cat# SA00001-2
Bacterial and virus strains		
Ubi-MCS-3FLAG-CBh-gcGFP-IRES-puromycin	Shanghai GeneChem Co.	N/A
hU6-MCS-CBh-gcGFP-IRES-puromycin	Shanghai GeneChem Co.	N/A
Chemicals, peptides, and recombinant proteins		
DMEM	Gibco™	Cat# 11885084
Fetal Bovine Serum	Gibco™	Cat# A5669701
PBS, pH 7.4	Gibco™	Cat# 10010023
0.25% Trypsin-EDTA (1X)	Gibco™	Cat# 25200072
Glucose, powder	Gibco™	Cat# 15023021
TRIzol™ Reagent	Gibco™	Cat# 15596018
RIPA Lysis Buffer	Servicebio	Cat# G2002
SDS-PAGE Sample Loading Buffer,5X	Beyotime	Cat# P0015
Critical commercial assays		
Cell Counting Kit-8	Beyotime	Cat# C0037
Human caspase-3 ELISA Kit	Bioswamp	Cat# HM10963
Human Bcl-2 ELISA Kit	Bioswamp	Cat# HM10524
One Step TUNEL Apoptosis Assay Kit	Beyotime	Cat# C1090
Pierce™ Rapid Gold BCA	Thermo Scientific™	Cat# A53226
RIPA Lysis Buffer	Servicebio	Cat# G2002
SurePAGE™, Bis-Tris, 4–12%	Genescript	Cat# M00654
Tris-MOPS-SDS Running Buffer Powder	Genescript	Cat# M00138
Thermo Scientific PageRuler	Thermo Scientific™	Cat# 26616
AceQ Universal U + Probe Master Mix V2	Vazyme	Cat# Q513-02
HiScript II 1st Strand cDNA Synthesis Kit	Vazyme	Cat# R211-01
Experimental models: Cell lines		
HLE-B3	ATCC	CRL-3603
Experimental models: Organisms/strains		
Mouse: C57BL/6	Charles River Laboratory	Wild type
Oligonucleotides		
Primers used for RT-qPCR, see Table S9	This paper	N/A

(*Continued on next page*)

Continued

REAGENT or RESOURCE	SOURCE	IDENTIFIER
Deposited data		
Mass spectrometry proteomics data of ACs	This paper	PRIDE: PXD059243
Software and algorithms		
Maxquant v.1.6.15.0	Max Planck Institute of Biochemistry	https://www.maxquant.org/
Skyline 21.2	MacCoss, University of Washington	https://skyline.ms/
ImageJ v.1.53	NIH	https://imagej.nih.gov/ij/
Prism v.9.0	San Diego	https://www.graphpad.com/scientific.software/prism/

EXPERIMENTAL MODEL AND SUBJECT DETAILS

Study participants and samples

We enrolled 20 patients with cataract who were undergoing treatment at the Hangzhou Branch of the Wenzhou Medical University Eye Hospital between February 2022 and May 2022. The patients were placed into two groups on the basis of their history of cataract and systemic diseases: those with ARC and those with DC. The patients with ARC did not have diabetes mellitus and all the cataracts that were present in patients with diabetes were defined as DC. The ACs were harvested during surgery and stored at −80°C prior to proteomic analysis. The exclusion criteria were as follows: (1) other eye diseases, such as glaucoma, ocular fundic disease, high myopia or acute inflammation of the eye; (2) systemic diseases other than diabetes; and (3) a history of eye surgery within the preceding 3 months. The study was approved by the Ethics Committee of the Eye Hospital of Wenzhou Medical University (no. H2024-020-K-15) and informed consent was obtained from all the participants. The study was performed in accordance with the principles of the Declaration of Helsinki and the Chinese Ministry of Health guidelines for sample collection from humans with diseases. Patient information is provided in Table S6.

Cell lines

Human lens epithelial cell lines (HLE-B3) (ATCC) were cultured in DMEM medium (5.5 mM glucose, Gibco, USA) supplemented with 10% fetal bovine serum (Gibco, USA) and 1% penicillin-streptomycin (Gibco, USA) at 37°C in a 5% CO2 environment. The identity of cells was confirmed by STR typing. At the same time, the cell lines were also tested for sterility and mycoplasma, and none of them were detected.We used Hoechst DNA staining (indirect), AGAR culture (direct), PCR-based tests for mycoplasma contamination. Once they reached 70%–80% confluence, the cells were incubated for 24 h in DMEM containing 5.5 mM, 50 mM, 100 mM, or 150 mM glucose.

Animals

Five-week-old male C57BL/6J mice were purchased from Charles River Laboratory, Zhejiang, China. The mice were housed in the Animal Center of Wenzhou Medical University under a 12-h light/dark cycle and provided with sterile water *ad libitum*. From 6 weeks of age, some mice were fed *ad libitum* with a high-fat diet (D12492) to establish DIO, and a control group was fed a standard diet. The criterion for successful establishment of the DIO model was a minimum mass of 32 g at 13 weeks of age (after 7 weeks of high-fat diet-feeding). DIO and control mice were weighed after feeding for 7 weeks (Table S7).

METHOD DETAILS

Sequencing and analysis

Liquid chromatography–mass spectrometry (LC-MS)

Samples were thawed, and the peptides were extracted and separated using an ultrahigh-performance liquid chromatography system. The peptides were then introduced into the NSI ionization source of an Orbitrap Exploris 480 (Thermo Fisher Scientific) mass spectrometer for analysis. Data acquisition was performed using a DIA program, alternating between primary and secondary mass spectrum analysis. The Homo database (20,389 sequences) was used for DIA data processing, along with the Spectronaut v 16.0 (Biognosys, Switzerland) search engine. The database used was Homo_sapiens_9606_SP_20230103.FASTA. Proteins with a fold difference in expression of >1.5 or <2/3 ($p < 0.05$) were defined as differentially expressed proteins (DEPs).

Parallel response monitoring (PRM) analysis

To verify the reliability of the proteomic data, 24 DEPs were selected for validation by PRM-targeted quantitative analysis. Enzymatically digested peptides were separated using a NanoElute ultra-performance liquid system, then secondary mass spectrometry data were obtained using Maxquant v.1.6.15.0 (Max Planck Institute of Biochemistry, Martinsried, Germany). An inverse library was used

to calculate the false positive rate (FDR) owing to random matching, and common contamination libraries were added to the database. The obtained MS data were processed using Skyline 21.2 (MacCoss, University of Washington).

Functional analysis

The Gene Ontology (GO) database (http://geneontology.org/) and the Kyoto Encyclopedia Gene and Genome (KEGG) database (http://www.genome.jp/kegg/pathway.html) were used for bioinformatic analyses. In addition, WoIF Psort software and PSORTb software (v3.0) were employed to predict the subcellular localization of prokaryotic and eukaryotic proteins. By means of comparison with the STRING (v.11.5) protein interaction network database, differential protein interactions with a confidence score >0.7 (high confidence) were identified. The R package ''visNetwork'' tool was then used to visualize the differential protein interaction network, using the 50 proteins with the closest interactions.

Cell culture and transfection

HLE-B3 were cultured in high-glucose Dulbecco's modified Eagle's medium

ted with 10% fetal bovine serum and 1x penicillin–streptomycin at 37°C with 5% CO2. HLECs were seeded into six-well plates, with 40,000 cells per well, and the cells were infected with lentiviral vectors (LVs). The GV493 RNA interference (RNAi) system (Shanghai GeneChem Co., Ltd.) was used to generate lentiviruses expressing short interfering RNA. LVs overexpressing SH2B1 were purchased from Shanghai GeneChem Co. Ltd. and were generated using the GV492 system. The gene number of SH2B1 was NM_001145795. The control groups of overexpressed and knockdown viruses were empty vectors. HLECs were infected at a MOI of 10 and cultured in DMEM medium for 3 days. HLEC cells stably overexpressing SH2B1 or with this gene knocked down were selected using puromycin (10 μg/mL). The siRNA sequences are shown in Table S8.

Quantitative polymerase chain reaction (q-PCR)

RNA was extracted from tissues and cells using TRIzol reagent (ThermoFisher, USA) and reverse transcribed using reverse transcriptase (Vazyme, China). Q-PCR analysis was conducted on a QuantStudio5 (Applied Biosystems, USA) using SYBR green Master Mix (Vazyme, China). The results were analyzed using the comparative threshold method ($2-\Delta\Delta Ct$), with GAPDH as the reference gene. The primers used are listed in Table S9.

Western blotting (WB)

Tissue and cellular lysates were prepared using RIPA containing phosphatase and protease inhibitors (Beyotime, China). Their total protein concentrations were determined using a BCA Protein Assay kit (Thermo Fisher, USA). Target proteins were separated on SDS-PAGE gels according to their molecular weight and transferred to PVDF membranes (Millipore, Burlington, USA). The membranes were then blocked with 5% nonfat milk for 1 h at room temperature and incubated with primary antibodies overnight at 4°C. Following incubation with HRP-labeled secondary antibody (Beyotime, China) for 1 h at room temperature, enhanced chemiluminescence (Nature Biosciences, China) was used to visualize specific bands. The protein band intensities were quantified using ImageJ software. All experiments were performed in triplicate.

Analysis of cell viability using a cell counting Kit-8 (CCK-8)

Cells (2×10^3/well) were seeded into 96-well cell culture plates and incubated for 12 h before incubation with high-glucose medium (100 mM) for 24, 48, and 72 h. Subsequently, 10 μL CCK-8 (Beyotime, China) and 90 μL DMEM were added to each well. After a 2-h incubation, the optical density (OD) of each well was measured at a wavelength of 450 nm using a microplate reader (Tecan, Switzerland) and the cell proliferation rate was calculated.

Wound healing assay

HLECs (1.5×10^4) were seeded in chambers on both sides of culture inserts (81176, IBIDI, Germany), which were removed after 12 h of cell attachment. Fresh DMEM containing 1% FBS was then added, and cells were incubated in an incubator. Cell migration was observed and photographed after 0 and 12 h using an EVOS700 microscope (Thermo Fisher, USA). ImageJ v.1.53 (NIH, USA) was used to calculate the scratch area. The extent of wound healing after 12 h was then calculated.

Elisa

Cell pellets were collected, washed with PBS, and lysed using an ultrasonic disruptor (Xiuilab, China). The cell debris was then removed, and the supernatants were stored at −80°C. ELISAs (Bioswamp, China) were performed according to the manufacturer's instructions. Standard curves were generated according to the concentrations and ODs of dilutions of the standards, and the sample concentrations were calculated using the ODs of the samples.

TUNEL fluorescence staining

Cells were seeded on cell slides and fixed with 4% PFA at 80% confluence. The cell slides were stained using a TUNEL kit (Yeason, China). Images (20×) were captured using a Pannoramic Midi (3DHistech, Budapest, Hungary), with a scale bar of 100 μm. The total number and number of TUNEL-positive cells were calculated for each image using ImageJ, and each experiment was performed in triplicate.

QUANTIFICATION AND STATISTICAL ANALYSIS

Prism v.9.0 (GraphPad, San Diego, CA, USA) was used for statistical analyses. Data are expressed as the mean ± SD or median (IQR). Student's t test was used for the analysis of continuous data with a normal distribution, whereas the Wilcoxon rank–sum test was used for analysis of non-normally distributed continuous data, and data reflecting more than two groups were analyzed using two-way ANOVA. Each experiment was performed at least in triplicate, and animal experiments were repeated on at least three independent occasions. $p < 0.05$ was considered to represent statistical significance.